

Preliminary rock physics analysis of basalts in the Lopra-1 well

Contribution to the SeiFaBa project
funded by the Sindri group

Gary Mavko, Peter Japsen,
and Lars Ole Boldreel



Preliminary rock physics analysis of basalts in the Lopra-1 well

Contribution to the SeiFaBa project
funded by the Sindri group

Gary Mavko¹, Peter Japsen²,
and Lars Ole Boldreel³

¹Stanford University, ²GEUS,
³University of Copenhagen

Contents

Data and stratigraphic interpretation	3
Rock physics analysis	3
Conclusions	10
References	11

Data and stratigraphic interpretation

A preliminary investigation of the rock physics properties of flood basalt on the Faroes has been carried out based on the extensive logging data from the Lopra-1/1A well. A detailed stratigraphy of basalt flows, sediment/tuff layers and dolerite dykes was established for the hole drilled in 1981 based on drill cuttings and cores and compared with the density, porosity, resistivity and gamma ray log-response (Hald & Waagstein 1984; Nielsen *et al.* 1984).

A more extensive logging program including a full wave sonic log was run in the deepened hole from 200 m to TD. The new logs have been used to establish a detailed stratigraphy for the flood basalt sequence between 200 m and 2500 m by dividing the lava flows into massive and porous parts (Boldreel 2003). The porous upper part of a flow is characterised by high values of the neutron porosity log, low values of density, low P- and S-velocities and intermediate values of the caliper. This in contrast to the rather massive part characterised by high values of density, high P- and S- wave velocities and low values of the neutron porosity. The basal zone is seldom identified due to the small vertical extent of the zone. In addition 52 intervals with >1% potassium were mapped at the flow boundaries and interpreted as altered basalt or tuffaceous sediments. These intervals were also identified from the high values of neutron porosity and caliper in combination with low values of density, P- and S-velocity. Two dolerite dikes intruding the basalt column were identified by having the highest values of density, P- and S-velocities and lowest values of the neutron porosity. The logs show that large differences exist in acoustic properties within the basalt column and we attribute these to significant variations in porosity – both in the form of vesicles and fractures – across each flow unit. This report presents some preliminary rock physics observations, as revealed by the logs of the Lopra-1 well (cf. Japsen *et al. in press*).

Rock physics analysis

Figure 1 shows a plot of the gamma ray, bulk density, P-wave velocity (V_p), the ratio of P-wave to S-wave velocities (V_p/V_s). The various facies that we will be discussing are color-coded (red = basalt topflows; blue = massive basalts; green = sediments; magenta = dolerites). We observe that the gamma ray curve shows systematically higher values for the sediments (green) and systematically lower values for the dolerite (magenta). The topflow and massive basalt facies have intermediate gamma ray values. The bulk density shows large fluctuations between about 1200 kg/m^3 and 3100 kg/m^3 . The high density limit of the curve is nearly constant with depth (except for a slight increase with depth), while the low density values are wildly fluctuating. We believe that the high bulk densities are asymptotically approaching the mineral density as the porosity approaches zero, while the low density values swing with porosity, as well as caliper anomalies. The P-wave velocities have wide fluctuations between about 3000 m/s and 7000 m/s, though there are systematic differences among the various facies. The sediments have the lowest velocities; the topflows have slightly higher velocities; the massive basalts are higher still; and the dolerites have the highest velocities.

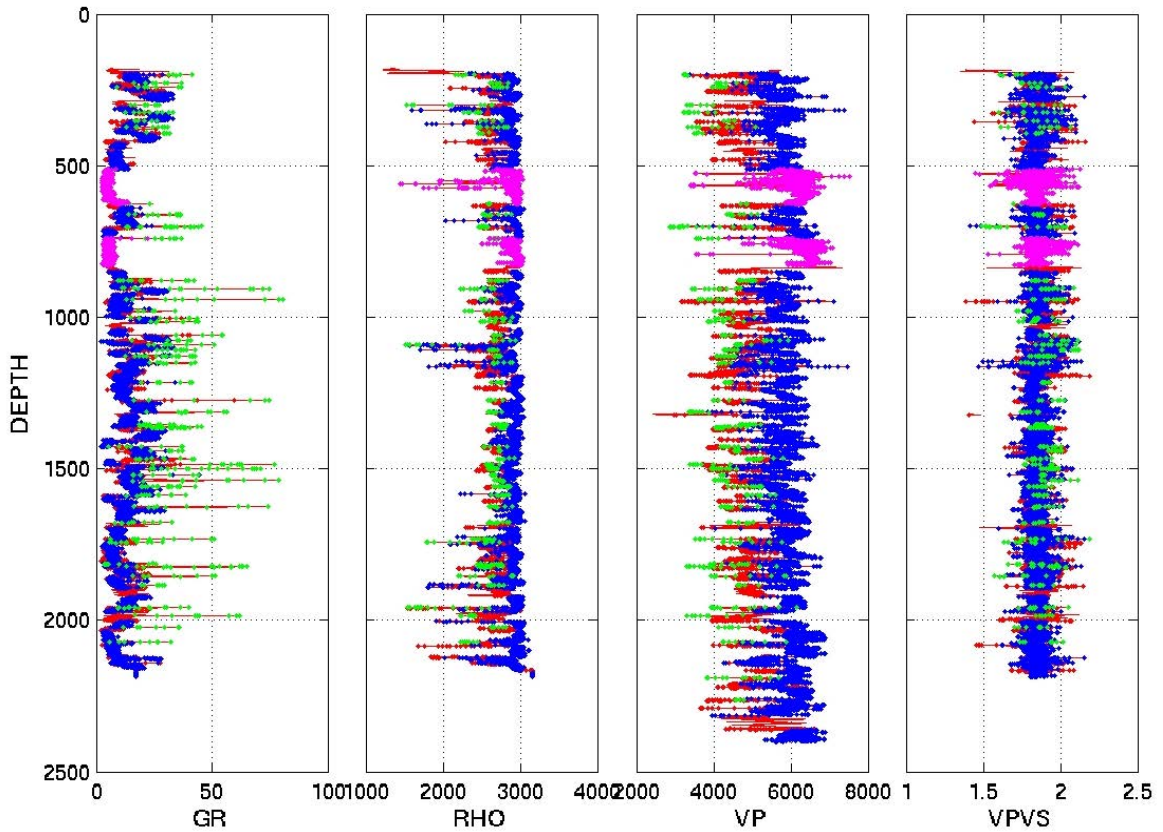


Figure 1. Well logs from Lopra-1. Facies are color-coded: red=basalt topflows, blue=massive flows, green=sediments, magenta=dolerite.

Figure 2 shows a crossplot of V_p vs. bulk density, again color coded by facies, as in Figure 1. The velocities increase consistently with density, with all four facies falling roughly along the same trend. We hypothesize that the primary parameter causing the large variations in velocity and density is porosity, both in the form of vesicles and fractures. The sediments and topflows, being most porous, have the lowest velocities and densities. The massive basalts span a large range of velocity and density (and therefore porosity), while the dolerites seismically resemble the lowest porosity basalts.

Superimposed on Figure 2 are empirical upper bounds on density and velocity (black lines), which we take as estimates of the mineral properties. The velocities and densities should asymptotically approach values appropriate for the minerals, as the porosity approaches zero.

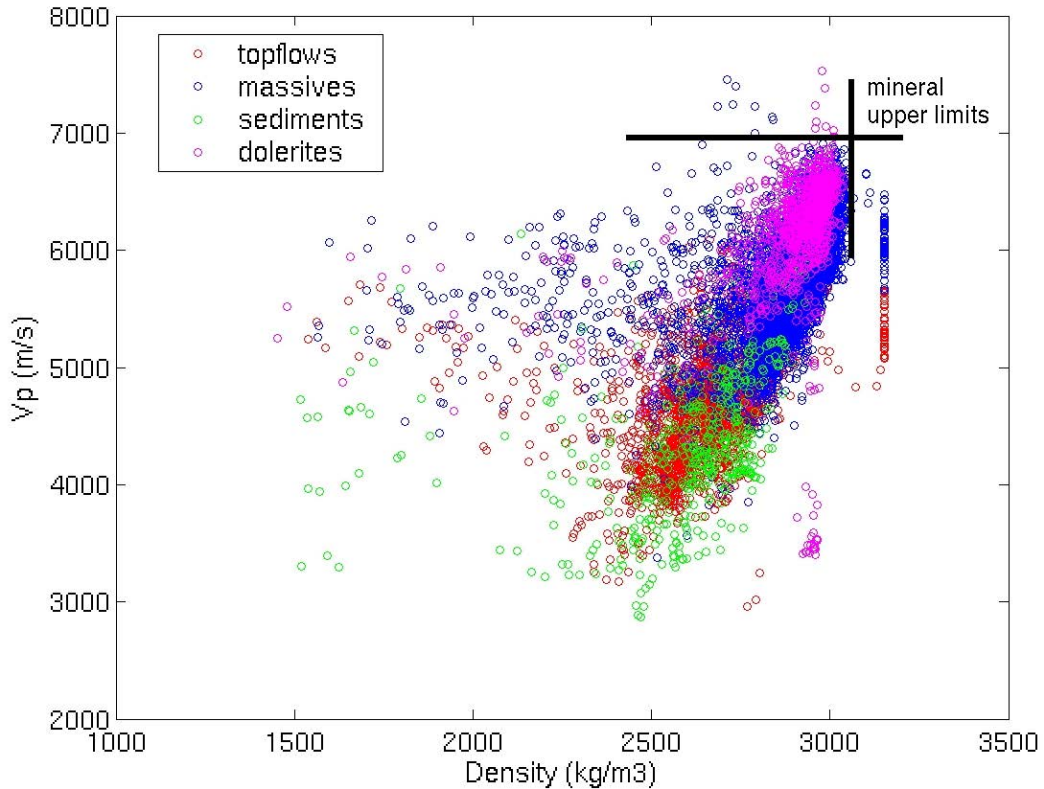


Figure 2. Crossplot of V_p vs. density from Lopra-1. Facies are color-coded: red=basalt topflows, blue=massive flows, green=sediments, magenta=dolerite. The black lines are empirical upper limits which we take as rough estimates of the mineral properties.

Table 1 shows some representative mineral properties (Mavko, et al., 1998). The empirical values of V_p and density drawn on Figure 2 are consistent with a mineral having properties similar to a mixture of plagioclase and pyroxene.

	Density (kg/m^3)	V_p (m/s)	V_s (m/s)	Bulk Modulus (GPa)	Shear Modulus (GPa)
Pyroxene (Augite)	3260	7220	4180	94	57
Plagio- clase (Al- bite)	2630	6460	3120	76	26
Olivine	3320	8450	491	130	80

Table 1. Physical Properties of Typical Rock-forming Minerals

Figure 3 shows a crossplot of V_p vs. neutron porosity, again color coded by facies, as in Figure 1. The velocities decrease consistently with increasing porosity, with all four facies falling roughly along the same trend. This supports the idea that porosity is the dominant parameter controlling the velocity. The sediments and topflows, being most porous, have the lowest velocities. The massive basalts span a large range of velocity and porosity, while the dolerites seismically resemble the lowest porosity basalts.

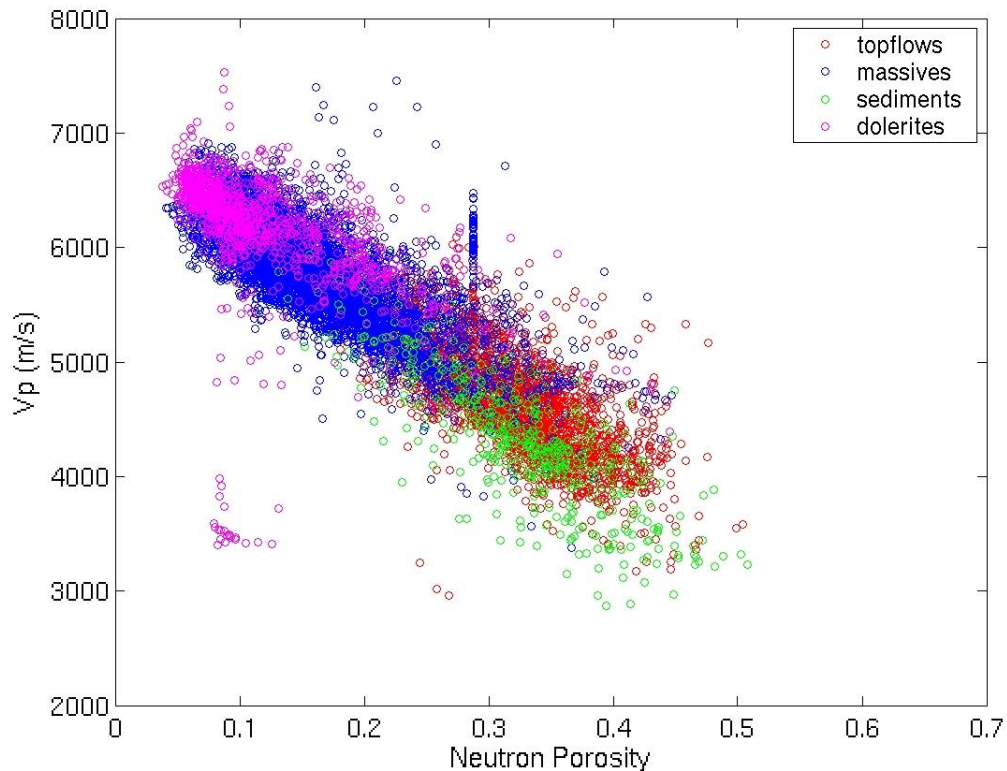


Figure 3. Crossplot of V_p vs. neutron porosity, from Lopra-1. Facies are color-coded: red=basalt topflows, blue=massive flows, green=sediments, magenta=dolerite.

Figure 4 shows the same crossplots of V_p vs. neutron porosity, as in Figure 3, except now the sediments are plotted separately from the basalts and dolerites. Superimposed on the plots are velocity-porosity models constructed using the Hashin-Shtrikman (1963) bounds. The upper and lower bounds define the range of physically possible velocities that a rock can have, given that its mineral has the properties of the left end member (at porosity zero) and that its pore fluid has the properties of the right end member (in this case, water). For the curves in Figure 4, we assumed mineral properties resembling pyroxene, from Table 1. The curved labeled “modified HS+” uses the functional form of the upper Hashin-Shtrikman bound, but it describes a mixture of mineral (left end member), and a suspension of mineral and water at the point where the porosity is large enough (“critical porosity”) that the rock is falling apart. Marion et al (1992) and Dvorkin and Nur (1996) have shown that the modified bounds are an effective way to describe the velocity-porosity trends for various rock types. We see in Figure 4 that the basalts and dolerites can be described with an empirical critical porosity of 0.6, while the sediments indicate a smaller critical porosity of 0.6. In general, granular materials tend to have a smaller critical porosity, while vesicular materials tend to have a larger critical porosity.

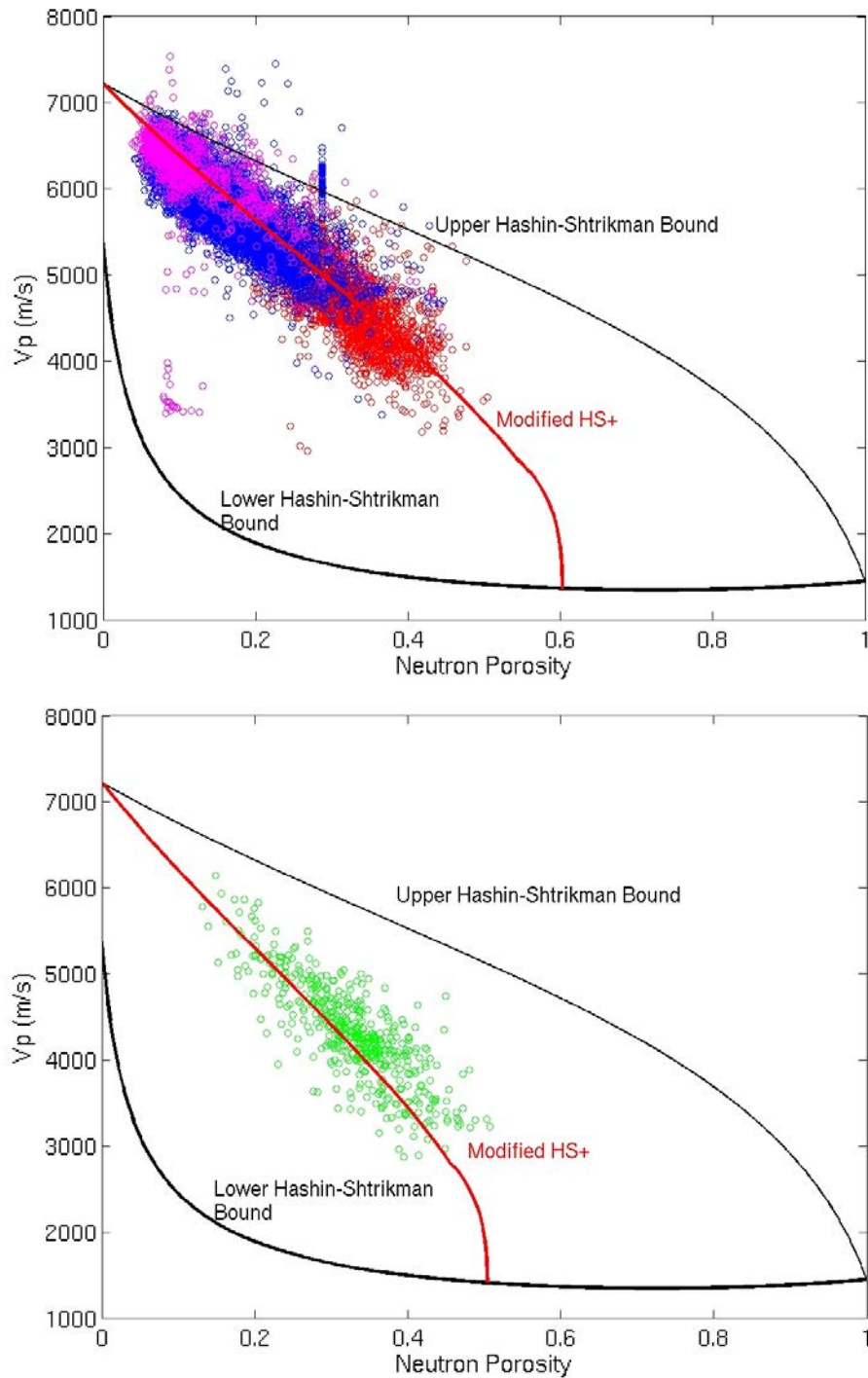


Figure 4. Crossplot of V_p vs. neutron porosity, from Lopra-1, as in Figure 3, with sediments separated from the basalts and dolerites. Facies are color-coded: red=basalt top-flows, blue=massive flows, green=sediments, magenta=dolerite.

Figure 5 shows the same data as in Figures 3 and 4. Here we superimpose effective medium models for velocity vs. porosity, computed using Berryman's (1980) formulation of the self-consistent approximation. For each of the four curves, the pores are assumed to take the shape of oblate spheroids, having aspect ratios 1, 0.3, 0.1, and 0.03, respectively. Again, the mineral is assumed to have properties similar to pyroxene, in Table 1, and the

pores are assumed to be filled with water. While spheroidal inclusion models are idealized, the trends of decreasing pore stiffness with decreasing aspect ratio make physical sense. Figure 5 suggests that the overall trends of the various facies in the Lopra-1 well can be represented with pores that are nearly spherical (aspect ratio 1) or slightly flattened (0.3), as one might expect for vesicular basalts. Those data that fall at velocities significantly below these trends are consistent with the occurrence of micro or macro fractures, which can be represented with very low aspect ratios.

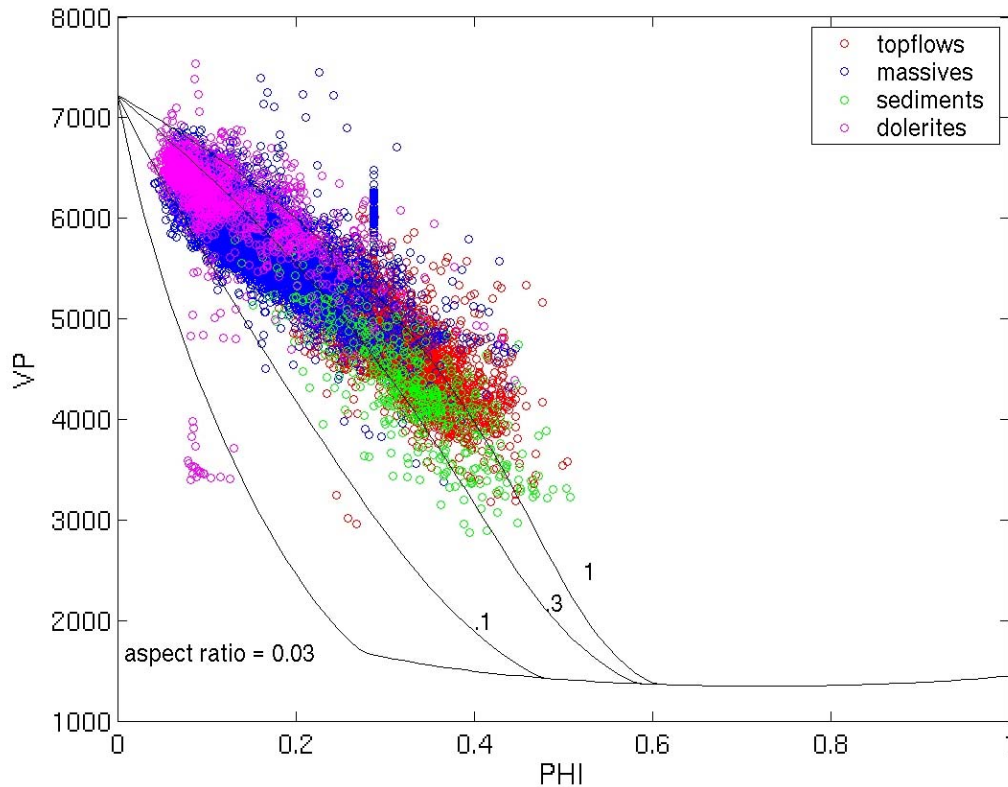


Figure 5. Crossplot of V_p vs. neutron porosity, from Lopra-1, as in Figure 3. Facies are color-coded: red=basalt topflows, blue=massive flows, green=sediments, magenta=dolerite. Solid black curves are effective medium models assuming ellipsoidal inclusions of 4 different aspect ratios.

Figure 6 shows crossplots of V_p vs. V_s for the same four facies of the Lopra-1 well. As is often the case, V_p and V_s are highly correlated. All four facies fall along the same narrow trend. High velocity points lying to the upper right can be interpreted as approaching the mineral values, while porosity increases along the trend to the lower left.

Superimposed on Figure 6 are empirical upper bounds on P- and S-wave velocities (black lines), which we take as estimates of the mineral properties, as in Figure 2. The velocities and densities should asymptotically approach values appropriate for the minerals, as the porosity approaches zero. These values are consistent with a mixture of pyroxene and plagioclase in Table 1.

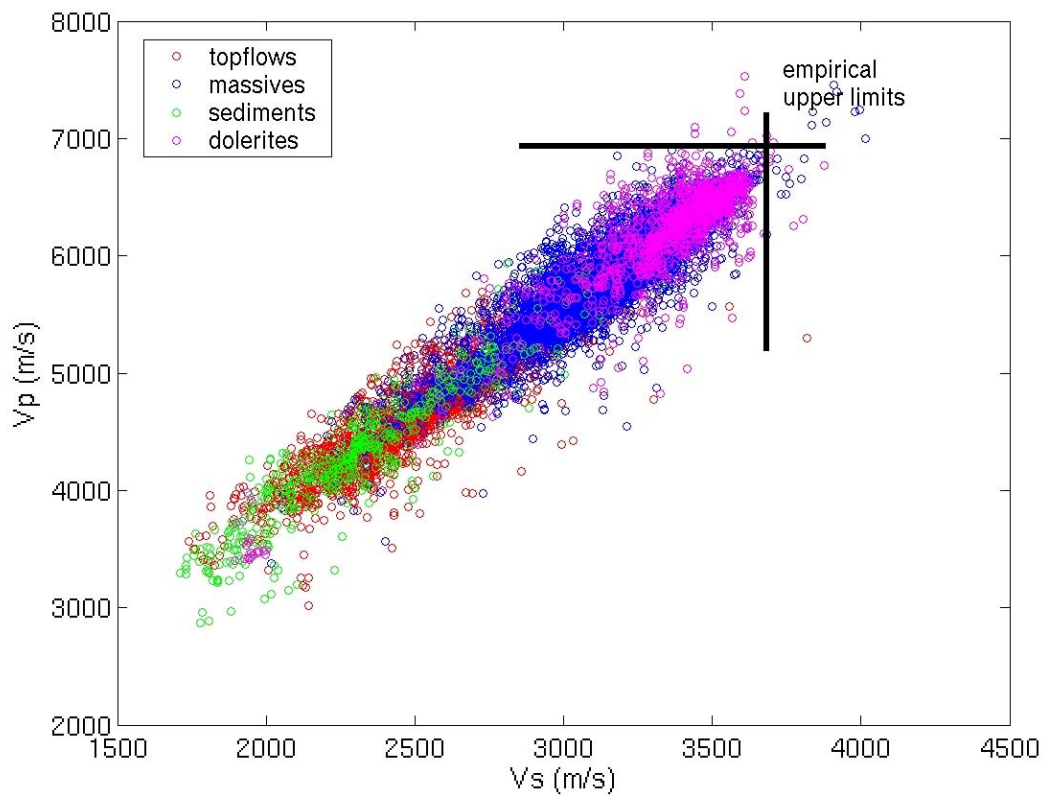


Figure 6. Crossplot of V_p vs. V_s , from Lopra-1. Facies are color-coded: red=basalt topflows, blue=massive flows, green=sediments, magenta=dolerite.

Figure 7 shows the same data as in Figure 6, but now we superimpose the Greenberg-Castagna (1992) empirical relations (black curves) and lines of constant Poisson's ratio (gray curves). While the Greenberg-Castagna relations were only derived for sedimentary rocks, it is useful to recall their features. In general, we expect that V_p and V_s will be highly correlated for a fixed composition. The high velocity ends of the empirical curves are dominated by the mineralogy, and the low velocity ends are dominated by the pore fluid. In Figure 7 we observe that the V_p and V_s for the four facies from the Lopra-1 well are well correlated. They fall along a trend similar to Dolomite and Limestone, with a mineral point resembling a mixture of pyroxene and plagioclase. They have a nearly constant Poisson's ratio of 0.3

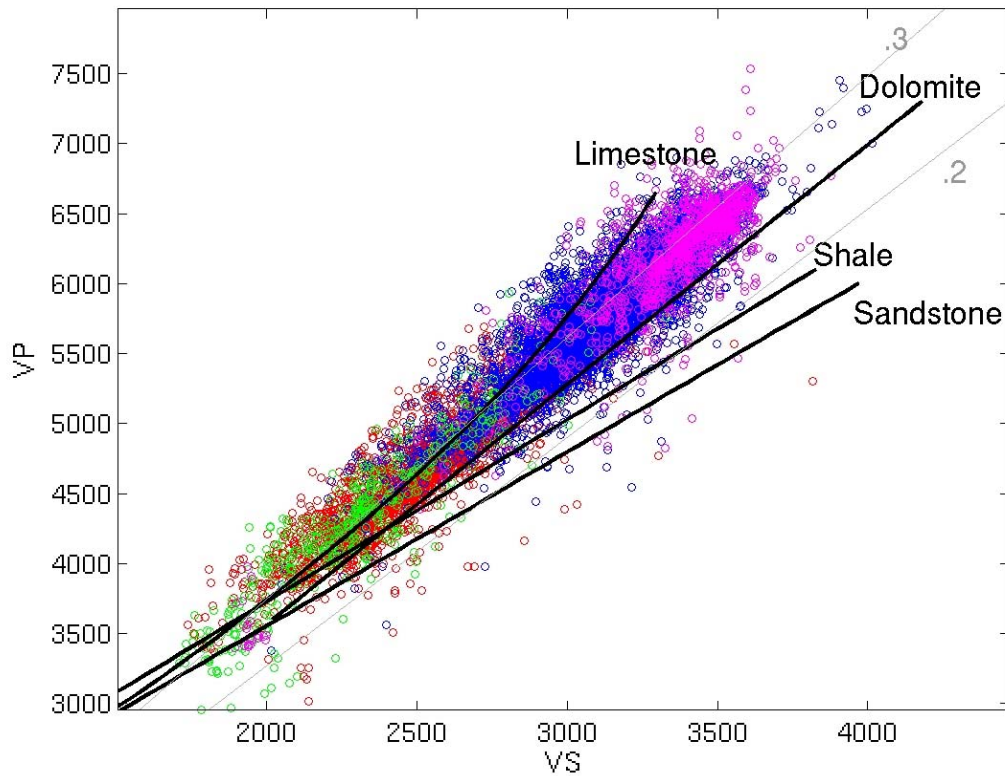


Figure 7. Crossplot of V_p vs. V_s , from Lopra-1, as in Figure 6. Facies are color-coded: red=basalt topflows, blue=massive flows, green=sediments, magenta=dolerite. Empirical Greenberg-Castagna lines are shown in black. Lines of constant Poisson's ratio are shown in light gray.

Conclusions

The preliminary analysis of log data from the flood basalts in the Lopra-1 well presented here suggests that the acoustic properties of these basalt flows are mainly controlled by porosity and the high correlation between P- and S-velocities may be indicative of a constant mineralogical composition for the Lower Basalt Formation. The new data acquired for the Upper and Middle Basalt formations in the Glyvursnes-1 and Vestmanna-1 may reveal how the acoustic properties of these formations differ from those of the Lower Basalt Formation (cf. Japsen et al *in press*).

References

- Berryman, J.G. 1980: Long-wavelength propagation in composite elastic media, I and II, *Journal of Acoustical Society of America* **68**, 1809-1831.
- Boldreel, L.O. 2003: Identification and characterization of basalt and sediment units based on wireline logs from the Lopra deep well, Faroe Islands, NE-Atlantic Ocean. EGS General Assembly XXVII Nice, France. Abstract EGS02-A-05330.
- Dvorkin, J. & Nur, A. 1996: Elasticity of high-porosity sandstones: Theory for two North Sea datasets. *Geophysics*, **61**, 1363-1370.
- Greenberg, M. & Castagna, J. 1992: Shear wave velocity estimation in porous rocks: Theoretical formulation, preliminary verification and applications, *Geophysical Prospecting*, **40**, 195-209.
- Hald, N. & Waagstein, R. 1984: Lithology and chemistry of a 2-km sequence of Lower Tertiary tholeiitic lavas drilled on Suduroy, Faroe Islands (Lopra-1). *In*: Berthelsen, O. Noe-Nygaard, A. & Rasmussen, J. (eds): *The deep drilling project 1980–1981 in the Faeroe Islands*. Føroya Frodskaparfelag, Torshavn, 15–38.
- Hashin, Z. & Shtrikman, S. 1963: A variational approach to the elastic behavior of multi-phase materials, *Journal of the Mechanics and Physics of Solids*, **11**, 127-140.
- Japsen, P., Andersen, C., Andersen, H.L., Boldreel, L.O., Mavko, G., Mohammed, N.G., Pedersen, J. M., Petersen, U. K., Rasmussen, R., Shaw, F., Springer, N., Waagstein, R., White, R. S. & Worthington, M. in press: Preliminary results of petrophysical and seismic properties of Faroes basalts (SeiFaBa project). *In*: Doré, A. G. & Vining, B. (eds): *Petroleum Geology: North-West Europe and Global Perspectives: Proceedings of the 6th Conference*. Geological Society, London.
- Marion, D., Nur, A., Yin, H. & Han, D-H. 1992: Compressional velocity and porosity in sand-clay mixtures, *Geophysics*, **57**, 554-563.
- Mavko, G., Mukerji, T. & Dvorkin, J. 1998: *The Rock Physics Handbook*, Cambridge University Press.
- Nielsen, P.H., Stefánsson, V. & Tulinius, H. 1984: Geophysical logs from Lopra-1 and Vestmanna-1. *In*: Berthelsen, O., Noe-Nygaard, A. & Rasmussen, J. (eds): *The deep drilling project 1980–1981 in the Faeroe Islands*. Føroya Frodskaparfelag, Torshavn.